

# National Institute of Technology ROURKELA



ONE YEAR RESEARCH PROJECT

*developed at*

DEPARTMENT OF CHEMISTRY, NATIONAL INSTITUTE OF TECHNOLOGY,  
ROURKELA

---

## Synthesis and Characterization of highly fluorescent multi-coloured Upconversion nanomaterials

---

*Author:*

Adhish SINGH

M.Sc.

Department of Chemistry

National Institute of Technology-Rourkela

*Supervisor:*

Dr. Supratim Giri

Assistant Professor

Department of Chemistry

National Institute of

Technology-Rourkela

2013-2015

---

# CERTIFICATE OF STUDY



## National Institute of Technology ROURKELA

This is certify that Mr. Adhish Singh, student of M.Sc. in Chemistry (2013-2015), in NIT Rourkela, Odisha, have carried out their dissertation work on “Synthesis and Characterization of highly fluorescent multi-coloured Upconversion nanomaterials ” under my supervision and guidance as a partial fulfillment of the degree of M.Sc. in Chemistry. The thesis embodies original work done by them and deserves merit for consideration for the degree. No results or any part of the result have been submitted anywhere for degree or equivalent qualification.

Date:

Dr. Supratim Giri

Place:

(Supervisor)

---

---

## ACKNOWLEDGEMENT

With deep regards and profound respect, we avail the opportunity to express our deep sense of gratitude and indebtedness to Prof. Supratim Giri, Department of Chemistry, National Institute of Technology, Rourkela, for introducing the present project topic and for his inspiring guidance, constructive criticism and valuable suggestions throughout the project work. We most gratefully acknowledge his constant encouragement and help in different ways to complete this project successfully.

We acknowledge our sincere regards to Prof. N. Panda (HOD, Dept. of Chemistry) and all the faculty members, Department of Chemistry, NIT Rourkela for their enthusiasm in promoting the research in chemistry and for their kindness and dedication to students. We would like to add a special note of thanks to Mr. Balmiki Kumar, Ph.D. Scholar, Department of Chemistry for his kind help and guidance whenever required.

We acknowledge the support of our classmates and lab mates throughout this course. Last but not the least, we take the privilege to express our deep sense of gratitude to our parents, for selflessly extending their ceaseless help and moral support at all time.

Adhish Singh

---

## ABSTRACT

The current research project work essentially deals with the synthesis of highly bright fluorescent nanoparticles which have the ability to emit wavelength shorter than that of the pumped wavelength. The synthesis was carried out using thermal decomposition method to dope lanthanide ions into the host lattice using lanthanum oxides as precursors. The Upconversion NPs formed were either capped by oleylamine or oleic acid, yielding their dispersibility in organic solvents and preventing them from agglomeration. We developed UCNPs having varied colours which can prove useful for barcoding and imaging purposes.

Further, we functionalised our NPs with silica using reverse micro-emulsion technique. These bifunctional nanocomposites increase the stability of upconversion materials and prevent the escape of rare earth ions from the lattice. The characterization for all the particles was carried out using XRD, EDAX, FTIR, DLS and Zeta potential analysis.

---

---

# Contents

<b>Certificate</b>	<b>i</b>
<b>1 Introduction</b>	<b>2</b>
1.1 Upconversion Nanoparticles (UCNPs)	2
1.2 Upconversion Mechanism	3
1.2.1 Excited State Absorption	3
1.2.2 Energy Transfer Upconversion	3
1.2.3 Photon Avalanche	4
1.3 Synthesis and Formation Mechanism of UCNPs	5
1.3.1 Thermal Decomposition	5
1.4 Upconversion Multicolour Tuning	5
1.5 Potential Applications	6
<b>2 Experimental</b>	<b>7</b>
2.1 Synthesis of UCNPs:	7
2.2 Synthesis of $\text{SiO}_2@\text{NaYF}_4: \text{Yb}^{3+}, \text{Er}^{3+}$	8
<b>3 Results and Discussion</b>	<b>9</b>
3.1 Characterization of UCNP	9
3.1.1 TEM and SAED pattern Analysis:	9
3.1.2 XRD analysis:	10
3.1.3 FTIR analysis:	10
3.1.4 TGA Analysis:	11
3.1.5 Photoluminescence Analysis:	12
3.2 Characterization of functionalized $\text{SiO}_2@ \text{NaYF}_4: \text{Yb}^{3+}, \text{Er}^{3+}$	12
3.2.1 XRD Analysis	12
3.2.2 FTIR Analysis	13
3.2.3 EDAX Analysis	14
3.2.4 DLS and Zeta potential analysis:	14
3.2.5 Photoluminescence analysis:	15
<b>4 CONCLUSION</b>	<b>16</b>

## Introduction

Upconversion (UC) phenomenon are non-linear optical process identified with the successive absorption of pump photons via metastable long-lived energy states followed by the emission at a shorter wavelength than the pump wavelength. This general concept was first recognized and formulated independently by Auzel, Ovsyankin, and Feofilov in the mid-1960s. [1]

They exhibit anti-Stokes luminescence, with both the excitation and emission wavelength commendatory for imaging purposes. By using near-infrared (NIR) light as the excitation source, up-conversion nanoparticles (UCNPs) have been studied widely because of its many advantages including the ability to penetrate deeply into tissue without causing any significant tissue damage, low autofluorescence, and good photostability.

### 1.1 Upconversion Nanoparticles (UCNPs)

During the past decade, upconverting nanoparticles (UCNPs) doped with rare earth ions have become a cardinal class of fluorescence contrast agents for imaging purposes. The upconversion phenomenon has been observed in d-block metals but importantly in the rare earth elements. Lanthanide (Ln) series [1].  $Ln^{3+}$  ions have  $4f^n 5d^{0-1}$  core configurations which is effectively shielded by outer shells electrons and have abundantly unique energy level structures. These  $Ln^{3+}$  ions can exhibit 4f-4f and 4f-5d transitions.

Upconversion nanoparticles consist of three major components: a host matrix, a sensitizer and an activator. [2] The sensitizer can be excited effectively from the energy of the incident light, which transfers this energy to the activator where emission is noticed. Therefore, the activator is the luminescence center in UCNPs, and the sensitizer enhances the luminescence efficiency. Both the ions are doped in insignificant quantity. The trivalent  $Yb^{3+}$  ion, which has a particularly simple energy level structure, is suitable for its use as sensitizer.  $Er^{3+}$ ,  $Tm^{3+}$  and  $Ho^{3+}$  ions have ladder like energy levels and thus function as UC activators. Recently, Liu's group along with others have focused on the surface modification and applications of lanthanum doped  $NaYF_4$  UCNPs. [2]-[6] Researchers reported that  $\beta$   $NaYF_4$ , the more thermodynamically stable form can be transformed from the  $\alpha$   $NaYF_4$ . Interestingly, we obtained the thermodynamically metastable  $\alpha$  phase of  $NaYF_4$  rather than the stable  $\beta$  phase because the free-energy barrier for the conversion from  $\alpha$   $NaYF_4$  to  $\beta$   $NaYF_4$  is very high, and thus requiring more energy for the transition from the cubic-to-hexagonal phase. [6]

Selection of host lattice: The host lattice can affect the UC efficiency in two ways:

1. by the phonon dynamics, and
2. by the local crystal field

Generally, larger is the number of phonons needed to convert the excitation energy into phonon energy, the lower is the efficiency of the nonradiative emission. Therefore in order to

enhance the emission efficiency by reducing the rate of non-radiative process, it is required to have the lanthanide ions embedded into a dielectric host of very low frequency phonons. RE fluorides importantly  $\text{AREF}_4$  ( $A=\text{Alkali}$ ) have been considered worthy host material due to their high refractive index and high transparency resulting from low energy phonons. A less symmetric crystal phase is mostly favourable for the upconversion puposes, as the inter-mixing of the lanthanide ion's f states with the higher electronic configurations can be better manifested. For example, hexagonal  $\text{NaYF}_4:\text{Yb}^{3+}/\text{Er}^{3+}$  nanocrystals exhibit visible upconversion photoluminescence, which is higher than its cubic geometry,[8] and monoclinic  $\text{ZrO}_2$  nanoparticles emit higher UC PL than the tetragonal phase nanoparticles.[9]

## 1.2 Upconversion Mechanism

UC processes are broadly divided into three categories: excited state absorption (ESA), energy transfer upconversion (ETU), and photon avalanche (PA). All these processes involve the simultaneous absorption of two or more photons.

### 1.2.1 Excited State Absorption

Excited-state absorption (ESA) is the sequential absorption of pump photons by a single ion due to the ladder-like electronic structure as illustrated in (Figure 1.1) by a three level system. When one ion or electron in the  $E_0$  state absorbs a photon, it is first excited to the  $E_1$  state; after absorbing the second photon, it can jump to the excited state  $E_2$  and emit higher energy photons while coming back to the ground state.

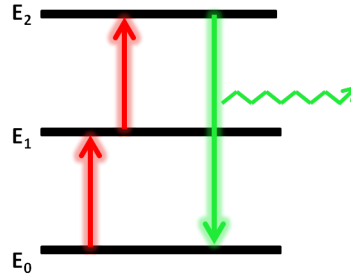


Figure 1.1: Excited State Absorption

### 1.2.2 Energy Transfer Upconversion

Energy Transfer Upconversion (ETU) is similar to ESA in that both processes utilize sequential absorption of two photons to populate the metastable level[1] as shown in the (Figure 1.2). The essential difference between ETU and ESA is that the excitation in ETU happens through energy transfer between two neighboring ions. In this process, electron transfer can take place in two different ways:

1. Resonant non-radiative transfer: When the distance between the ions are near enough and the excited energies of sensitizer (S) and activator (A) are nearly equal, energy can be transferred from S to A, and simultaneously exciting A from its ground state to excited state before S emits photons.
2. Phonon-assisted non-radiative transfer in two-ion-involved system.

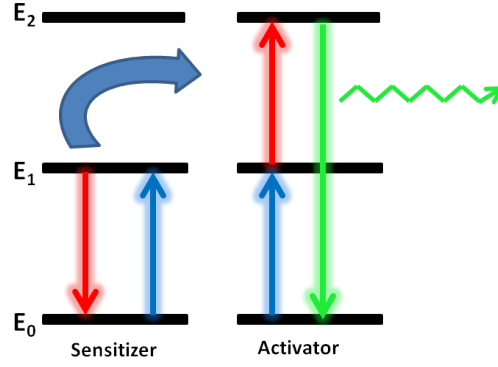


Figure 1.2: Energy Transfer Upconversion

### 1.2.3 Photon Avalanche

Photon avalanche (PA) in (Figure 1.3) is a process that produces upconversion above a certain threshold of excitation power. Below the threshold, little of up-converted fluorescence is seen, while the PL intensity increases by orders of magnitude above the pump threshold. The excitation radiation is generally not resonant with the absorption transition from the ground state to the intermediate states, but a little higher than  $E_2$ . Through the process of cross relaxation, it goes down to  $E_2$  state. Energy transfer occurs between the  $E_2$  state electron and the  $E_0$  state electron. This results in the formation of two electrons in the  $E_1$  state. One of them absorbs the excitation wavelength and gets excited to the  $E$  state, where it interacts with  $E_0$  state electrons and energy transfer occurs to form three  $E_1$  electrons. However, in this case the excitation radiation is resonant with the absorption transition from  $E_1$  to  $E$ . By following the same steps again, the number density of electrons in the  $E$  state increases dramatically. When these electrons go back to the  $E_0$  state, high-energy photons are emitted.

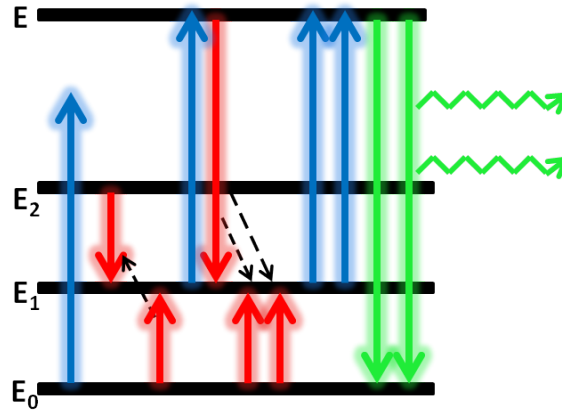


Figure 1.3: Photon Avalanche



### 1.3 Synthesis and Formation Mechanism of UCNPs

A variety of chemical techniques, including coprecipitation, thermal decomposition, hydro(solvo)thermal synthesis, sol-gel processing and combustion synthesis, have been demonstrated to synthesize lanthanide-doped UC nanocrystals.

Techniques		
Method	Hosts	Remarks
Co-precipitation	LaF <sub>3</sub> NaYF <sub>4</sub> LuPO <sub>4</sub>	Fast growth treatment with cheap equipments
Thermal Decomposition	LaF <sub>3</sub> NaYF <sub>4</sub> GdOF	Expensive, air sensitive precursors. Monodisperse NC. Toxic byproducts
Solvothermal Synthesis	LaF <sub>3</sub> YVO <sub>4</sub>	Cheap raw materials. Excellent control over particle size
Sol-gel	ZrO <sub>2</sub> TiO <sub>2</sub> BaTiO <sub>3</sub>	Cheap raw materials, Calcination at high temperature required
Combustion Technique	Y <sub>2</sub> O <sub>3</sub> Gd <sub>2</sub> O <sub>3</sub> La <sub>2</sub> O <sub>3</sub>	Energy economic. Time savvy. Particle aggregation
Flame Synthesis	Y <sub>2</sub> O <sub>3</sub>	Time efficient.

Out of all the listed methods, Thermal Decomposition is being followed widely.

#### 1.3.1 Thermal Decomposition

As it is known that metallic trifluoroacetates can effortlessly thermally decompose to their corresponding metal fluorides[10]. For example, lanthanum trifluoroacetates (La(CF<sub>3</sub>COO)<sub>3</sub>). Since the discovery, this method has become an easy and familiar way of synthesizing high quality doped NaYF<sub>4</sub> UCNPs. A general synthesis of high-quality Na(RE)F<sub>4</sub> (RE = Y, Pr to Lu) NPs using Na(CF<sub>3</sub>COO) and RE(CF<sub>3</sub>COO)<sub>3</sub> as precursors has been reported by Mai et al[6]. The solvents were chosen which could act as a coordinating solvent and noncoordinating solvent. Next, 1-octadecene (ODE) with a high boiling point 315 °C was used as the noncoordinating solvent to provide a high-temperature environment. While Oleic acid (OA) and oleyamine (OM), which can coordinate effectively, was taken as the coordinating solvent which prevented agglomeration by capping the surface of NPs.

### 1.4 Upconversion Multicolour Tuning

The ability to manoeuvre Upconversion emission colour is highly crucial for their application in biological labelling and barcoding.

1. By changing the relative amount of dopant ions and host material, we can change the emission wavelength and their relative intensity.[10]. The coupling between f-f transition and the local crystal field of the host lattice is quite weak and hence can be exploited to obtain change in relative emission intensity. However, phonon distribution from the host lattice and surface ligands can produce a significant change in the population density between two closely spaced energy level of a given lanthanide ion.
2. Size-dependent luminescence property results from surface effects instead of quantum effects because of small radius of the exciton in the lanthanide-doped nanocrystals. As the size of nanoparticle gets reduced, the concentration of surface dopant ions is steadily increased. The emission spectrum of the nanocrystals is a sum of emissions from dopant ions at the surface and in the interior of the particles. Size of the nanocrystals can be controlled to regulate the concentration of surface dopant ions, leading to a gradual change in the colour produced.
3. The relative amount of the dopant ions and the average distance between neighboring dopant ions influences the optical properties of the nanocrystals[11]. For example, an

increase in the concentration of  $\text{Yb}^{3+}$  in  $\text{Y}_2\text{O}_3:\text{Yb}/\text{Er}$  nanoparticles brings about an enhanced back-energy transfer from  $\text{Er}^{3+}$  to  $\text{Yb}^{3+}$ , thus leading to a relative increase in intensity of red emission of  $\text{Er}^{3+}$ [12].

4. It is now known that numerous surface and bulk defects could exist as an outcome of the low-temperature synthesis and the high surface area of nanoparticles.[13]. Few defects could lead to formation of nonradiative recombination centers which results in quenching of excited  $\text{Er}^{3+}$  states[14]. With increase in temperature the shapes of UCNP become more and more regular[15].

## 1.5 Potential Applications

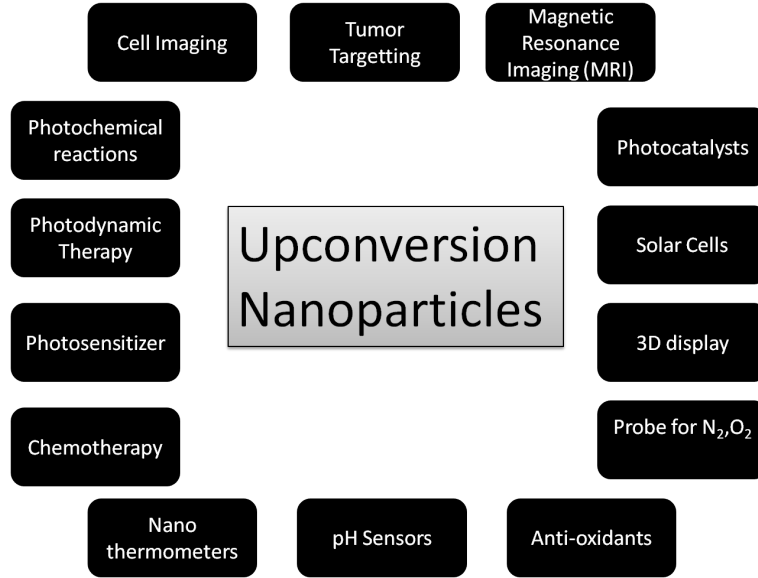


Figure 1.4: Applications of UCNP

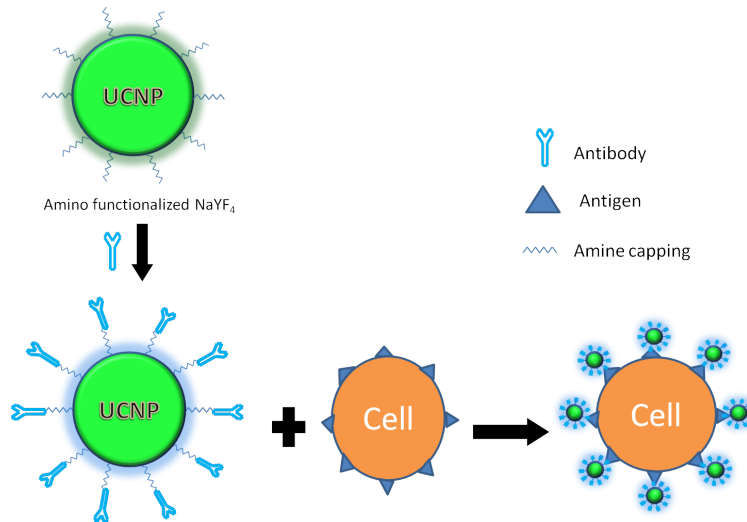


Figure 1.5: Mechanism for the immunolabeling[16]–[17]

## Experimental

**Materials:** The rare-earth oxides including yttrium oxide ( $\text{Y}_2\text{O}_3$ , > 99.99%), ytterbium oxide ( $\text{Yb}_2\text{O}_3$ , > 99.99%), thulium oxide ( $\text{Tm}_2\text{O}_3$ , > 99.99%), holmium oxide ( $\text{Ho}_2\text{O}_3$ , > 99.99%) and erbium oxide ( $\text{Er}_2\text{O}_3$ , > 99.99%), Oleic acid (OA, 90%), octadecene (ODE, 90%), tetraethylorthosilicate (TEOS), were purchased from Sigma-Aldrich, ammonia ( $\text{NH}_3$ , 25%) was purchased from SD-Fine Chemicals, Triton-X100 was purchased from HI-MEDIA and Ethanol was purchased from CSS Chemicals. All chemicals were analytical grade and used as received without further purification. The DI water used in the experiment was purified by a Millipore system.

### 2.1 Synthesis of UCNPs:

Yb and Er co-doped  $\text{NaYF}_4$  nanoparticles (Y: Yb: Er = 78%:20%:2%) stabilized with oleic acid (OA) were synthesized by a modified thermal decomposition method[19] as shown in the (Figure 2.1) . In the followed procedure, 0.975 mmol of yttrium(III) oxide ( $\text{Y}_2\text{O}_3$ ), 0.25 mmol of ytterbium(III) oxide ( $\text{Yb}_2\text{O}_3$ ) and 0.025 mmol of erbium(III) oxide ( $\text{Er}_2\text{O}_3$ ) were dissolved in 8 ml 50% aqueous trifluoroacetic acid (TFA) in a 250 ml two-necked flask. The solution was then heated to 80 °C with vigorous magnetic stirring for 120 minutes to remove water and residual TFA. Next, 1mL of DI water was added to the flask and homogenised through sonication. 2.5 mmol (340mg) sodium trifluoroacetate ( $\text{NaCOOCF}_3$ , 98%) was added, along with 9.0 mL of oleic acid (OA) and 9.0 ml of 1-octadecene (ODE). The solution was put under vacuum so as to evacuate any dissolved oxygen and water and then heated at 100 °C. Subsequently, the solution was purged with argon and heated at the rate of 30 °C  $\text{min}^{-1}$  and maintained at 330 °C for 60 minutes to obtain the NCs. The NCs were thoroughly washed with ethanol (EtOH) and chloroform ( $\text{CHCl}_3$ ) two to three times.

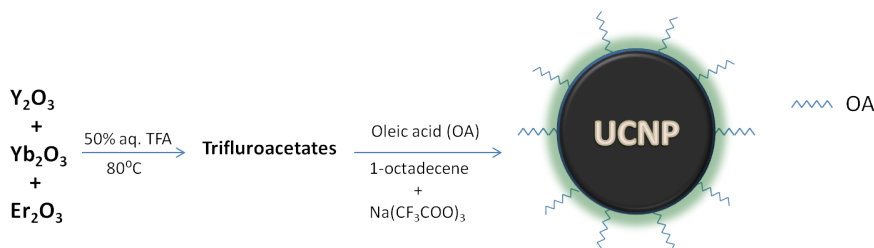


Figure 2.1: Synthesis of UCNP

The UCNPs were well dispersed in a nonpolar solvent (*e.g.*, cyclohexane, chloroform, dichloromethane) without any detectable agglomeration. With the hydrophobic oleic acid capping ligand, the as prepared UCNPs have no intrinsic aqueous solubility. Therefore, surface functionalization with hydrophilic materials is required prior to the biomedical applications.

## 2.2 Synthesis of $\text{SiO}_2@\text{NaYF}_4: \text{Yb}^{3+}, \text{Er}^{3+}$

- (a) **Step 1: Preparation of Triton-X100 functionalised UCNPs:** Using reverse microemulsion is a facile strategy for silica coating of NPs, and thus a modified reverse microemulsion method [18] was developed for the surface modification of the as prepared NPs. Triton TX-100 (20 mL) and  $\text{NaYF}_4:\text{Yb}^{3+}, \text{Er}^{3+}$  nanocrystals (0.1 g) were mixed in a glass container under ultrasonication for 10 mins. to form a transparent solution. 80 mL of water was added with stirring at room temperature for 6 h before it was collected by centrifugation and washed with deionized water several times.
- (b) **Step 2: Functionalization of UCNPs by  $\text{SiO}_2$ :** The precipitate obtained after the above step were dispersed into a mixed solution of 160 mL of ethanol, 3 mL of water, and 0.5 mL of ammonia (28%); the solution was stirred at room temperature for 6 h while 0.01 mL of TEOS was slowly added dropwise. Finally, the product was collected by centrifugation and washed with deionized water and ethanol several times and dried in lyophiliser at  $-55^\circ\text{C}$  for 24 h.

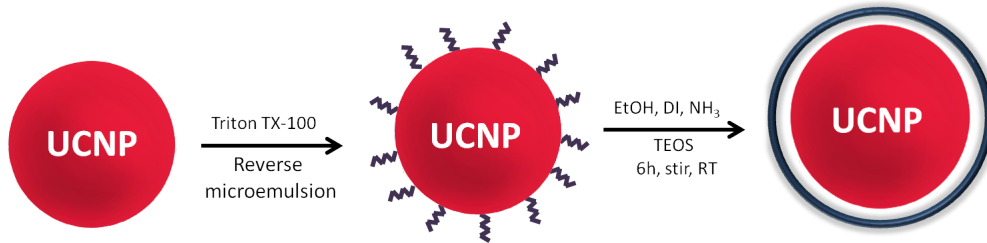


Figure 2.2: Synthesis of  $\text{UCNP}@\text{SiO}_2$

## Results and Discussion

**Characterization:** Scanning electron microscopy (SEM) was conducted in FEI-FESEM (Nova nano SEM) operated at 5 kV with gold coating for 2 min. Fourier transform infrared analysis (FTIR) was done using a Perkin-Elmer FTIR Spectrometer. UV-vis absorbance was measured using Shimadzu, UV-2450 Spectrophotometer. TEM was carried in JEOL 3010, Japan operated at 300 kV. TGA was carried out using STA449C/4/MFC/G/ Netzsch, Germany at heating rate of 10 °C/min in presence of air atmosphere and a complementary argon flow was used as a protective gas. Visible photoluminescence images were taken with a handheld 980 nm laser with 0.005 Watt source.

### 3.1 Characterization of UCNP

#### 3.1.1 TEM and SAED pattern Analysis:

Synthesis of oleylamine coated  $\text{NaYF}_4$  nanoparticles doped with  $\text{Yb}^{3+}$  (20%) and  $\text{Er}^{3+}$  (2%) have been carried out by the thermal decomposition method. The detailed characterisation of the synthesised upconversion nanoparticle with  $\text{Er}^{3+}$ ,  $\text{Ho}^{3+}$  and  $\text{Tm}^{3+}$  as dopant have been shown in Figure 3.1.

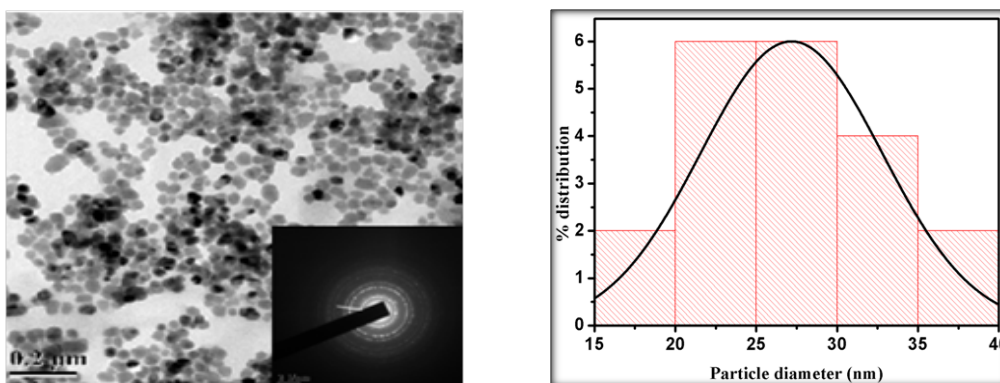


Figure 3.1: TEM and SAED pattern of upconversion materials. a)  $\text{NaYF}_4:\text{Yb}^{3+}$ ,  $\text{Er}^{3+}$  b) Size distribution curve for oleylamine capped  $\text{NaYF}_4:\text{Yb}^{3+}$ ,  $\text{Er}^{3+}$ .

The synthesized UCNPs exhibited size ranging from 20 nm to 30 nm. The TEM image of the material showed that the synthesized nanoparticles are approximately 25 nm, which is corroborated by plotting the size distribution curve from the TEM image. Also, the SAED pattern unequivocally supports the crystallinity of the as synthesised nanoparticle.

### 3.1.2 XRD analysis:

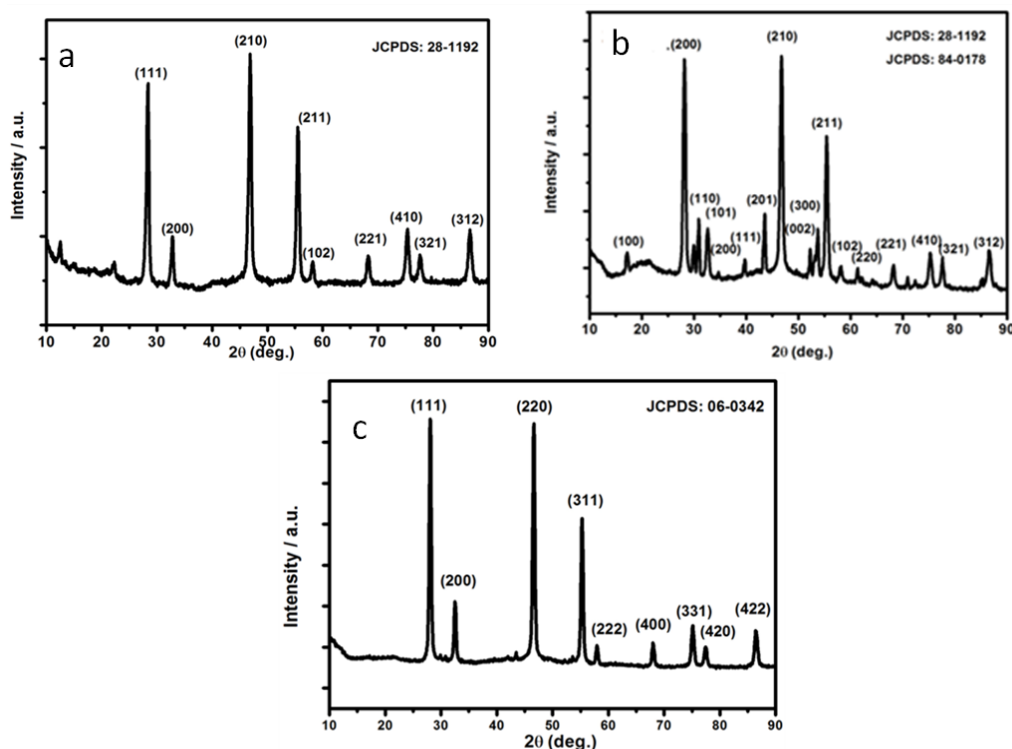


Figure 3.2: XRD of UCNPs a)  $\text{NaYF}_4:\text{Yb}^{3+}, \text{Er}^{3+}$  b)  $\text{NaYF}_4:\text{Yb}^{3+}, \text{Ho}^{3+}$  c)  $\text{NaYF}_4:\text{Yb}^{3+}, \text{Tm}^{3+}$

The crystalline nature of the material was demonstrated by the X-ray diffraction. The lattice parameters demonstrated identical base structure of  $\text{NaYF}_4$  as evident from the powder X-ray diffraction pattern (Figure 3.2). The peak positions indicate the formation of  $\text{NaYF}_4$  crystal lattice structure. This diffraction pattern matched with that of standard JCPDS data. This diffraction pattern is little different from that of  $\text{Er}^{3+}$  doped UC material due to the presence of  $\text{Ho}^{3+}$  as one of the dopant ions.

### 3.1.3 FTIR analysis:

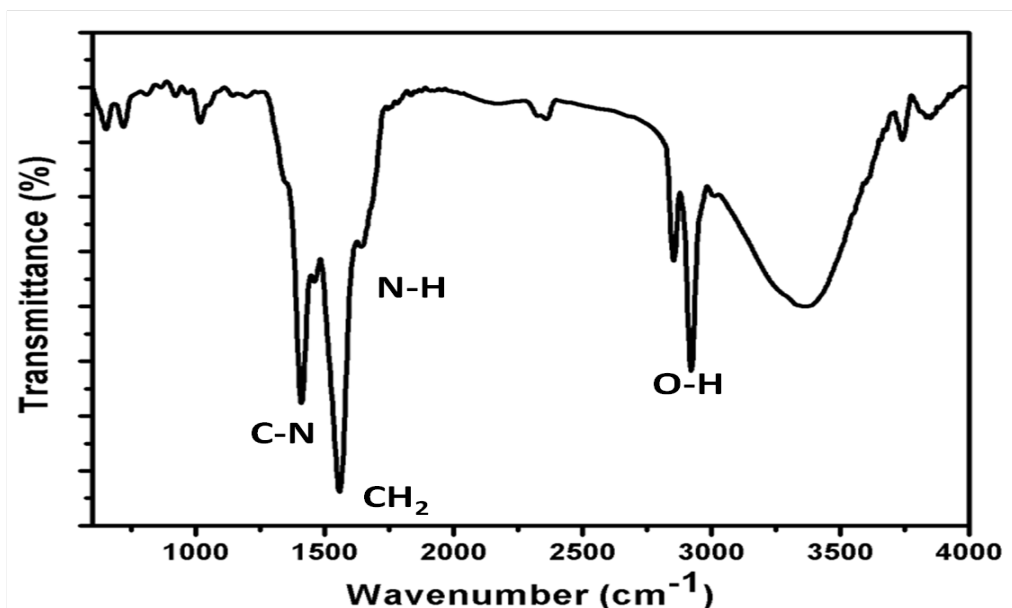


Figure 3.3: FTIR spectra of Oleylamine capped  $\text{NaYF}_4:\text{Yb}^{3+}, \text{Er}^{3+}$

The oleylamine coating of the UCNPs was further confirmed by the FTIR spectra (Figure 3.3), where characteristic peaks for N-H bond stretch and C-H bond stretch of oleylamine molecule is explicitly visible at around  $3300\text{ cm}^{-1}$  and  $2900\text{ cm}^{-1}$ , respectively.

### 3.1.4 TGA Analysis:

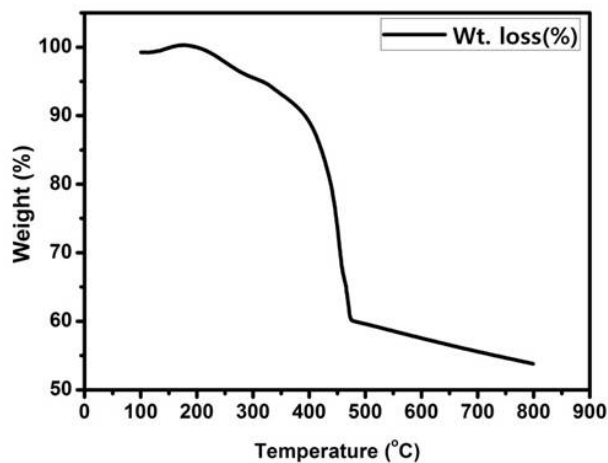


Figure 3.4: TGA of Oleylamine capped  $\text{NaYF}_4:\text{Yb}^{3+}, \text{Er}^{3+}$

From the figure (Figure 3.4), it is quite evident that the oleylamine coated magnetic nanoparticles are quite stable up to temperatures as high as  $350^\circ\text{C}$ . The initial weight loss at temperature below  $400^\circ\text{C}$  refers to the evaporation of oleylamine. The sharp loss of weight around  $500^\circ\text{C}$  corresponds to the complete loss of oleylamine capping from the surface of the  $\text{NaYF}_4:\text{Yb}^{3+}, \text{Er}^{3+}$  UCNP.

### 3.1.5 Photoluminescence Analysis:

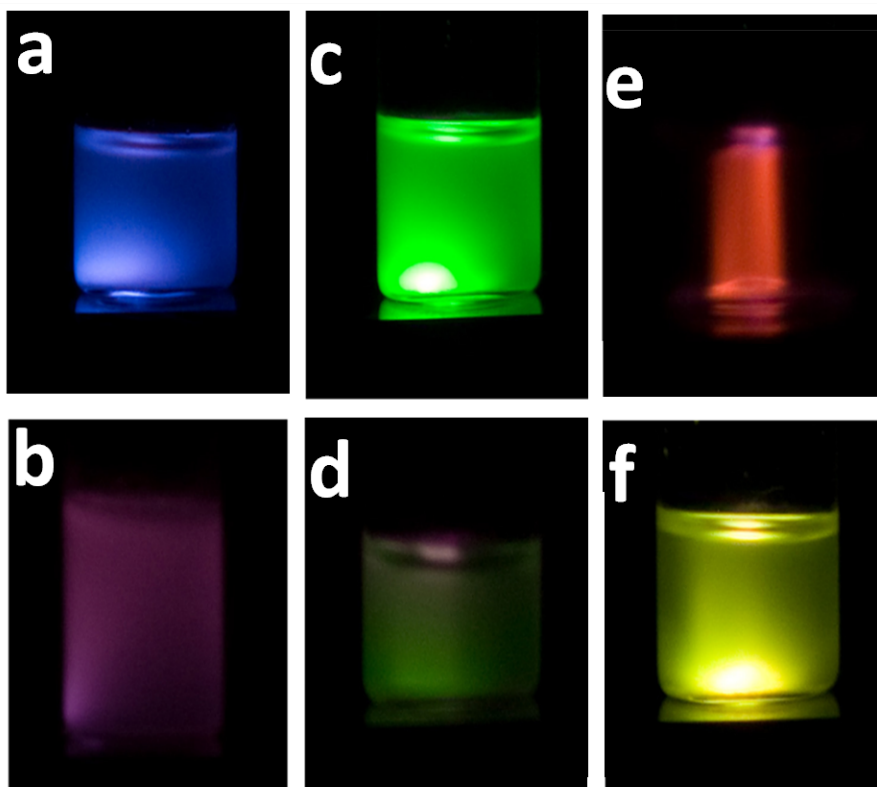


Figure 3.5: Photoluminescence images of upconversion materials. a)  $\text{NaYF}_4:\text{Yb}^{3+},\text{Tm}^{3+}$  b)  $\text{NaYF}_4:\text{Yb}^{3+},\text{Ho}^{3+}$  c)  $\text{NaYF}_4:\text{Yb}^{3+},\text{Er}^{3+}$  UCNPs.

## 3.2 Characterization of functionalized $\text{SiO}_2@\text{NaYF}_4:\text{Yb}^{3+},\text{Er}^{3+}$

### 3.2.1 XRD Analysis

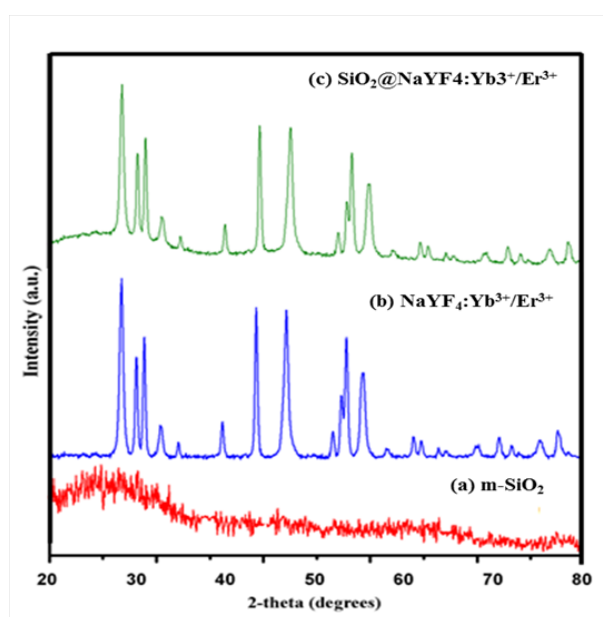


Figure 3.6: XRD Plot of a) mesoporous Silica b)  $\text{NaYF}_4:\text{Yb}^{3+},\text{Er}^{3+}$  UCNP c)  $\text{SiO}_2@\text{NaYF}_4:\text{Yb}^{3+},\text{Er}^{3+}$  UCNP



XRD was carried out to determine the crystal structure of the as prepared silica functionalised UCNPs. The XRD patterns of the  $\text{NaYF}_4:\text{Yb}^{3+},\text{Er}^{3+}$  NCs are shown in (Fig. 3.6, The XRD pattern clearly resembles the JCPDS data 16-0334 available in the database for  $\text{NaYF}_4$ . It is to be noted that the XRD pattern clearly demonstrates the existence of mainly hexagonal structures; however, the additional diffraction peaks at about 2-theta degrees of  $28^\circ$  (111),  $31^\circ$  (200) basically correspond to cubic-phase crystals. This phenomenon of co-existence of hexagonal and cubic phase of the nanoparticles is attributed to the relationships between reaction conditions (reactant concentration, hydrothermal time) and nanocrystals properties (size, crystallization, shape, phase transformation).[20]

### 3.2.2 FTIR Analysis

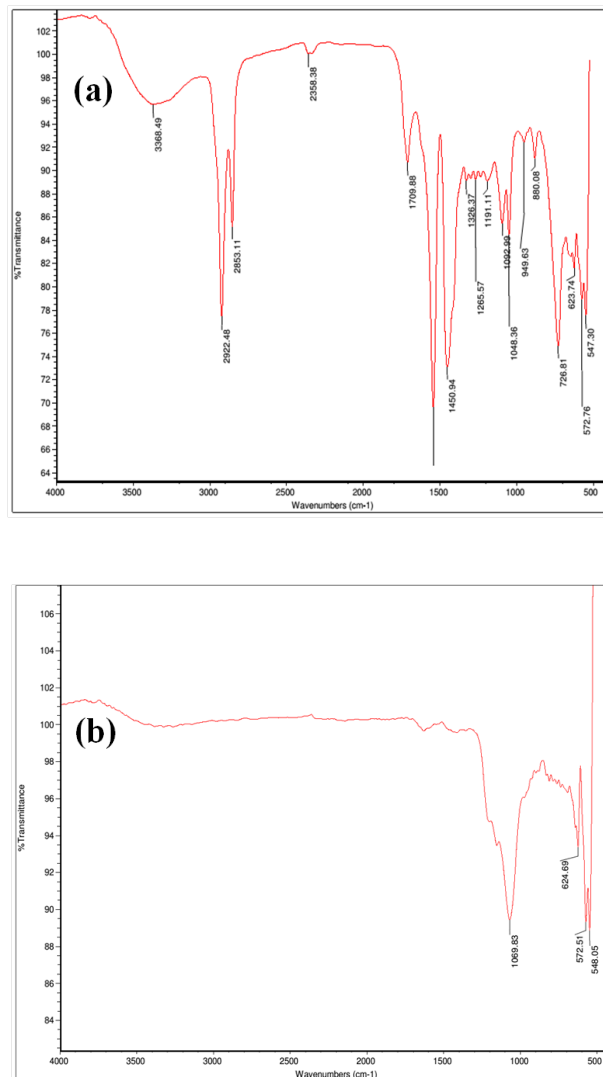


Figure 3.7: : FTIR spectra of a) Oleic acid capped  $\text{NaYF}_4:\text{Yb}^{3+},\text{Er}^{3+}$  b) Silica functionalized  $\text{NaYF}_4:\text{Yb}^{3+},\text{Er}^{3+}$

The FTIR spectra of  $\text{NaYF}_4:\text{Yb}^{3+},\text{Er}^{3+}$  NCs. The absorption at around  $3421\text{ cm}^{-1}$  in the spectrum of the nanoparticle is assigned to the O-H stretching vibration in a  $-\text{COOH}$  group, and the bands at  $2924$  and  $2854\text{ cm}^{-1}$  can be attributed to the asymmetric and symmetric stretching vibration modes, respectively, of methylene ( $-\text{CH}_2-$ ) groups in the long alkyl chain of the oleic acid molecule. The strong peak at  $1565\text{ cm}^{-1}$  can be assigned to the asymmetric stretching vibrations of the carboxylate group, and the  $1464\text{ cm}^{-1}$  peak results from the symmetric stretching vibrations of the carboxylate group ( $-\text{COO}-$ ). These data, corresponding to the oleic acid, confirm that the oleic acid was in fact on the nanoparticle surface used as the surfactant to control the size and shape of the  $\text{NaYF}_4:\text{Yb}^{3+},\text{Er}^{3+}$  NCs. FTIR spectra of  $\text{SiO}_2@\text{NaYF}_4:\text{Yb}^{3+},\text{Er}^{3+}$  nanocomposite coated with a layer of silica

were measured to demonstrate that silica was successfully wrapped upon the nanoparticle  $\text{NaYF}_4:\text{Yb}^{3+},\text{Er}^{3+}$  (Fig. 3.7). The absorption bands due to  $-\text{OH}$  ( $3428\text{ cm}^{-1}$ ) and  $\text{H}_2\text{O}$  ( $1633\text{ cm}^{-1}$ ) are clear. The strong peaks at  $1091$  and  $801\text{ cm}^{-1}$  can be attributed to the asymmetric and symmetric stretching vibration modes of the  $\text{Si}-\text{O}-\text{Si}$  group, respectively. The  $947\text{ cm}^{-1}$  peak results from the symmetric stretching vibrations of the  $\text{Si}-\text{OH}$  group. The intensity of the bands around  $3445\text{ cm}^{-1}$  ( $-\text{OH}$ ) and  $1629\text{ cm}^{-1}$  ( $\text{H}_2\text{O}$ ) reveal that a large number of  $\text{O}-\text{H}$  groups present on the silica coat over the prepared nanoparticle. Thus, the FTIR characterisation unequivocally establishes shows silica coatings on the surface of the upconversion nanoparticle was successfully prepared.

### 3.2.3 EDAX Analysis

EDAX analysis establishes the composition of silica functionalised upconversion nanoparticle, exhibiting peaks for Na, Er, Yb, Y, Si, O, while the presence of Au is attributed to the gold coating done while analysis.(Figure 3.8)

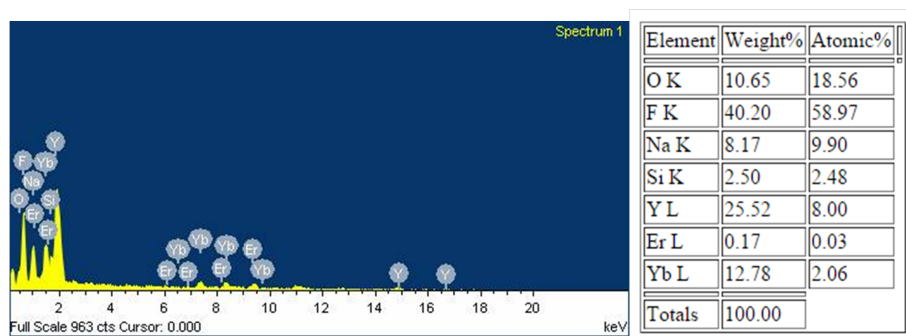


Figure 3.8: EDAX of  $\text{SiO}_2@\text{NaYF}_4:\text{Yb}^{3+},\text{Er}^{3+}$  UCNPs

### 3.2.4 DLS and Zeta potential analysis:

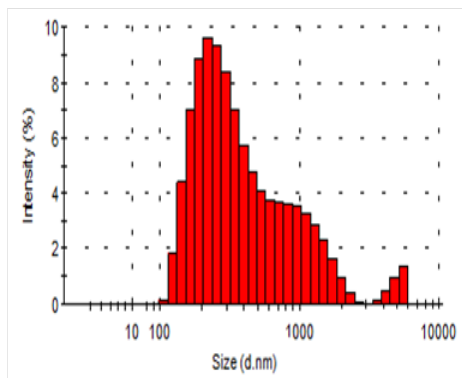


Figure 3.9: DLS Size Distribution

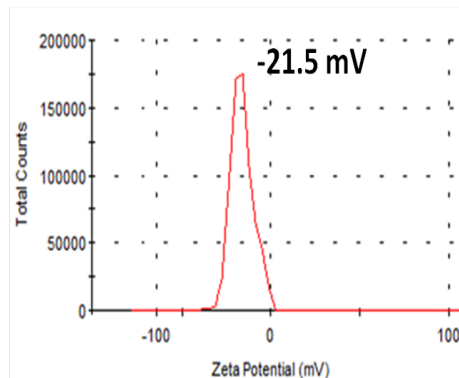


Figure 3.10: Zeta Potential Analysis

Dynamic light scattering (DLS) analysis, shown in Fig. 3.9, determined the hydrodynamic particles size distribution profile of synthesized  $\text{SiO}_2@\text{NaYF}_4:\text{Yb}^{3+}/\text{Er}^{3+}$  nanoparticles. In our result, the size of prepared Silica functionalized  $\text{NaYF}_4:\text{Yb}^{3+},\text{Er}^{3+}$  NPs is found to be in nanometer range.

The zeta potential distribution analysis, shown in fig. Fig. 3.10, was carried out to determine the surface charge of the as prepared  $\text{SiO}_2@\text{NaYF}_4:\text{Yb}^{3+}/\text{Er}^{3+}$ ; and it was found that the material exhibited the surface charge of  $-21.5\text{ mV}$ , which is typical to the silica surface due to the presence of free  $-\text{OH}$  groups, establishing the silica coat on the UCNPs surface.

### 3.2.5 Photoluminescence analysis:



Figure 3.11: Photoluminescence of Silica functionalized UCNP (a) before and (b) after irradiation with 980nm hand held laser

The UC photoluminescence of the as-prepared  $\text{NaYF}_4$  UCNPs is dictated by the co-doped  $\text{Yb}^{3+}$  and  $\text{Er}^{3+}$  ions: the  $\text{Yb}^{3+}$  ion act as a sensitizers which absorbs at 980 nm NIR excitation radiation without any visible UC emission, and the  $\text{Er}^{3+}$  ion act as an activators emitting visible UC photoluminescence, characteristic of their atomic transitions, leading to the green emission, as shown in the Fig. 3.11

---

## CONCLUSION

The present work was carried out to investigate the synthesis and characterization of bright highly luminescent upconversion nanoparticles. The NPs can be synthesized from  $M_2O_3$  (where,  $M=Yb, Y, Er, Ho, Tm$ ) using thermal decomposition technique. In a concise way, we demonstrated how such bright and beautiful coloured upconversion materials can be synthesized simply by modulating few parameters like temperature, composition and other reaction conditions like decomposition time. This kind of synthesis allows us to play with the kind of phase we desire for the particles and the phases, in turn, affecting the emission characteristic of the particle.

Further, we carried out functionalization of UCNPs where we capped the NP within the silica leading to increased stability of the particles. Upon analysis by XRD and FTIR, it was evident that the silica got capped onto the surface of upconversion nanoparticles.

This work has serious potential to be applied in various areas, such as bioimaging, photodynamic therapy, nanosensors, solar cells and drug delivery to list few. Also, the hydroxyl group of silica can be easily functionalized with other groups to serve useful applications. These characteristics once exploited can have various prospects in the future.

---

---

## Bibliography

- [1] F. Auzel. *Auzel*. Chem. Rev., 2004, 104, 139.
- [2] Wang F, Liu XG. *Recent advances in the chemistry of lanthanide-doped upconversion nanocrystals* Chem Soc Rev 2009;38:976-89.
- [3] Vetrone F, Capobianco JA. *Lanthanide-doped fluoride nanoparticles: luminescence, upconversion, and biological applications* Int J Nanotechnol 2008;5:1306-39.
- [4] Wang F, Banerjee D, Liu YS, Chen XY, Liu XG. *Upconversion nanoparticles in biological labeling, imaging, and therapy* Analyst 2010;135:1839-54.
- [5] Li CX, Lin J. *Rare earth fluoride nano-/microcrystals: synthesis, surface modification and application* J Mater Chem 2010;20:6831-47. 15. Bunzli JCG. Lanthanide luminescence for biomedical analyses and imaging. Chem Rev 2010;110:2729-55.
- [6] Mai HX, Zhang YW, Si R, Yan ZG, Sun LD, You LP, et al. *High-quality sodium rare-earth fluoride nanocrystals: controlled synthesis and optical properties* J Am Chem Soc 2006;128:6426-36.
- [7] Wang F, Han Y, Lim CS, Lu YH, Wang J, Xu J, et al. *Simultaneous phase and size control of upconversion nanocrystals through lanthanide doping*. Nature 2010;463:1061-5.
- [8] Kramer, K. W.; Biner, D.; Frei, G.; Gudel, H. U.; Hehlen, M. P.; Luthi, S. R. Chem. Mater. 2004, 16, 1244
- [9] Patra, A.; Friend, C. S.; Kapoor, R.; Prasad, P. N. Appl. Phys. Lett. 2003, 83, 284
- [10] S. Heer, K. Kompe, H. U. Gudel and M. Haase Adv. Mater., 2004, 16, 2102
- [11] Dan Li, Biao Dong, Xue Bai, Yu Wang, and Hongwei Song *Influence of the TGA Modification on Upconversion Luminescence of Hexagonal-Phase NaYF<sub>4</sub>:Yb<sup>3+</sup>, Er<sup>3+</sup> Nanoparticles* J. Phys. Chem. C 2010, 114, 8219–8226
- [12] F. Vetrone, J. C. Boyer, J. A. Capobianco, A. Speghini and M. Bettinelli J. Am. Chem. Soc., 2006, 128, 7444
- [13] A. Huignard, T. Gacoin and J. P. Boilot Chem. Mater., 2000, 12, 1090
- [14] S. M. Lee, Y. Jun, S. N. Cho and J. Cheon J. Am. Chem. Soc. 2002, 124, 11244
- [15] Wenbin Niu, Suli Wu, Shufen Zhang and Lian L *Synthesis of colour tunable lanthanide-ion doped NaYF<sub>4</sub> upconversion nanoparticles by controlling temperature* Chem. Commun., 2010, 46, 3908–3910
- [16] Wang M, Mi CC, Wang WX, Liu CH, Wu YF, Xu ZR, et al. *Immunolabeling and NIR-excited fluorescent imaging of HeLa cells by using NaYF<sub>4</sub>:Yb,Er upconversion nanoparticles*. ACS Nano. 2009; 3:1580–6.
- [17] Wang M, Mi CC, Zhang YX, Liu JL, Li F, Mao CB, et al. *NIR-responsive silica-coated NaYbF<sub>4</sub>:Er/Tm/Ho upconversion fluorescent nanoparticles with tunable emission colors and their applications in immunolabeling and fluorescent imaging of cancer cells*. J Phys Chem C. 2009; 113:19021–7.
- [18] Shiyong Yu, Jing Zhao, Xuechuan Gao, Renfei Zhang, Zhibing Tan and Haiquan Su *Bifunctional dual-modal luminescence nanocomposites: grafting down luminescence onto core-shell, up-conversion silica nanoarchitecture* RSC Adv., 2014, 4, 33749

- [19] Shiyong Yu, Jing Zhao, Xuechuan Gao, Hui Jing and Haiquan Su *A synthesis and up-conversion photoluminescence study of hexagonal phase  $\text{NaYF}_4\text{:Yb,Er}$  nanoparticles* CrystEngComm, 2013, 15, 10100-10106
- [20] Y. J. Sun, Y. Chen, L. J. Tian, Y. Yu, X. G. Kong, J. W. Zhao and H. Zhang, Nanotechnology, 2007, 18, 275609.